Behaviour of and mass transfer at gas-evolving electrodes

Electrochimica Acta, Vol. 34, No. 2, pp. 161–169, 1989.
Printed in Great Britain.

0013–4686/89 $3.00+0.00

BEHAVIOUR OF AND MASS TRANSFER AT GAS-EVOLVING ELECTRODES

L. J. J. JANSSEN

Laboratory for Electrochemistry, Faculty of Chemical Technology, Eindhoven University of Technology, P.O. Box 513, 5600 MB Eindhoven, The Netherlands

(*Received* 3 *March* 1988; *in revised form* 16 *June* 1988)

Abstract—A complete set of models for the mass transfer of indicator ions to gas-evolving electrodes with different behaviour of bubbles is described theoretically.

Sliding bubbles, rising detached single bubbles, jumping detached coalescence bubbles and ensembles of these types of bubbles are taken into consideration as well as the behaviour of various types of bubbles, in particular, the detached coalescence bubble is discussed.

The set of models is checked using literature data of mass-transfer coefficients for ferricyanide ions and ferrocyanide ions to, respectively, a hydrogen-evolving and an oxygen-evolving electrode in alkaline solution under conditions of forced convection of solution. It has been found that the mass transfer of indicator ions to various types of gas-evolving electrodes can be described well by the set of models proposed.

NOMENCLATURE

a_1, a_2	proportionality factors
A_d	average cross-section of detached bubbles; bubble cross-section (m^2)
A_e	surface area of electrode (m^2)
A_p	electrode surface area coming into contact with the effective track of a smoothly detached rising single bubble (m^2)
A_s	electrode surface area coming into contact with the track of a slipping bubble (m^2)
A_w	electrode surface area coming into contact with fresh bulk solution after the jump detachment of a bubble (m^2)
c_b	concentration of indicator ion in bulk solution (mol m^{-3})
c_0	c_x at $x=0$ (mol m^{-3})
c_x	concentration of indicator ion at distance x from electrode surface area (mol m^{-3})
D	diffusion coefficient of indicator ion (m^2 s^{-1})
F	Faraday constant, $= 9.6487 \cdot 10^7$ C $kmol^{-1}$
i	electric current density (kA m^{-2})
I	electric current (kA)
k	mass transfer coefficient of the indicator ion to the electrode surface (m s^{-1})
k_e	mass transfer coefficient of the indicator ion i obtained by extrapolation of k–i curve (m s^{-1})
k_f	mass transfer coefficient of the indicator ion at forced convection in absence of gas-bubble evolution to the electrode surface (m s^{-1})
k_p	k under convectionless conditions for the electrode surface A_p (m s^{-1})
$k_{p,a}$	average value of k_p for period t_p (m s^{-1})
k_s	k under convectionless conditions for electrode surface A_s (m s^{-1})
$k_{s,a}$	average value of k_s for period t_s (m s^{-1})
k_{sp}	k for electrode surface A_s+A_p (m s^{-1})
k_{sw}	k for electrode surface A_s+A_w (m s^{-1})
k_w	k under convectionless conditions for electrode surface A_w (m s^{-1})
$k_{w,a}$	average value of k_w for period t_w (m s^{-1})
m	number of moles of the indicator ion diffusing to an electrode surface per unit of time (mol s^{-1})
m_p	m for electrode surface A_p (mol s^{-1})
$m_{p,1}$	m_p during period t_p (mol s^{-1})
$m_{p,2}$	m_p during period t_d-t_p (mol s^{-1})
$m_{p,3}$	$m_{p,1}+m_{p,2}$ (mol s^{-1})
m_s	m for electrode surface A_s (mol s^{-1})
$m_{s,1}$	m_s during period t_s (mol s^{-1})
$m_{s,2}$	m_s during period t_d-t_s (mol s^{-1})
$m_{s,3}$	$m_{s,1}+m_{s,2}$ (mol s^{-1})
m_{sp}	$m_{s,3}+m_{p,3}$ (mol s^{-1})
m_{sw}	$m_{s,3}+m_{w,3}$ (mol s^{-1})
m_w	m for electrode surface A_w (mol s^{-1})
$m_{w,1}$	m_w during period t_w (mol s^{-1})
$m_{w,2}$	m_w during period t_d-t_w (mol s^{-1})
$m_{w,3}$	$m_{w,1}+m_{w,2}$ (mol s^{-1})
N	number of detached bubbles per unit surface area and time (cm^{-2} s^{-1})
n	number of bubbles on a picture or on part of a moving film
n	*number of electrons, involved in the reaction to* form one molecule of a species
n_1, n_2	proportionality factors
R	radius of bubble (m)
R_d	average radius of departed bubbles; bubble radius (m)
$R_{d,i}$	radius of the departed bubble i (m)
$R_{S,d}$	Sauter bubble radius; $R_{S,d}=3V_d/4A_d$ (m)
s_1	length of the track of a sliding bubble (m)
s_2	effective length of the track of a rising detached single bubble (m)
t	time (s)
t_d	bubble cycle time (s)
t_p	time, $t_p=(\alpha_3 R)^2/\pi D$ (s)
t_s	time, $t_s=(\alpha_1 R)^2/\pi D$ (s)
t_w	time, $t_w=D/\pi k_f^2$ (s)
t_1	time $D/\pi k_f^2$ (s)
T	temperature (K)
v_g	volumetric gas production rate (m s^{-1})
$v_{g,b}$	volumetric production rate of gas bubbles (m s^{-1})
$v_{g,0}$	volumetric production rate of gas bubbles when all the gas is evolved as bubbles (m s^{-1})
v_s	solution flow velocity (m s^{-1})
V_d	average volume of departed bubbles; bubble volume (m^3)

V_M volume of 1 mol gas; 24.4×10^{-3} at 298 K ($m^3\ mol^{-1}$)
x distance from the electrode surface (m)
$\alpha_1, \alpha_2, \alpha_3$ proportionality factors
β enhancement factor for mass transfer $[(k - k_f)/k_f]$
δ_f thickness of Nernst diffusion layer (m)
η_b efficiency of gas bubble evolution

Subscripts

a average value
b bubbles, bulk
d detached bubble
e electrode; extrapolated
f forced convection
g gas
H hydrogen
i indicator ion i
O oxygen
p rising detached single bubble
s sliding bubble; solution
w jumping detached bubble
x distance from the electrode surface

1. INTRODUCTION

Electrolytic gas evolution is a significant phenomenon in most electrochemical processes in applied electrochemistry. Electrolytically evolved bubbles enhance transport of heat or mass at gas-evolving electrodes. In particular, the mass transfer of indicator ions to a gas-evolving electrode has been extensively studied. Recently, Vogt[1] and Sides[2] have published thorough surveys.

Different models have been proposed to describe the mass-transfer coefficient k, of an indicator ion to a gas-evolving electrode. The applicability of the various models depends to a considerable extent on the occurrence or non-occurrence of coalescence of bubbles formed during gas evolution[3]. A penetration model[4] and a convection-penetration model[3] are proposed for a gas-evolving electrode with coalescing bubbles at, respectively, natural and forced convection of solution. A hydrodynamic model[5] and, recently, a modified hydrodynamic model[6] are presented for a gas-evolving electrode without the occurrence of coalescence. This paper presents an advanced hydrodynamic-penetration model, which is useful for different types of gas-evolving electrodes. Various aspects of previous models are incorporated in the new model. Experimental results already published are used to verify the usefulness of the new model.

2. THEORY

The rate of mass transfer of indicator ions to a gas-evolving electrode is described by a new model in which the enhancement of mass transfer by bubbles slipping over the electrode surface and/or detaching from the electrode surface are taken into account. The formation, growth, slip and detachment of a bubble requires a time, t_d, called the bubble cycle time. It is assumed that this phenomenon is constantly repeated on the same area of the electrode surface after a time t_d.

A bubble departs from its nucleation site, slides a distance s_1 over the electrode surface and after that, detaches from the electrode surface. The sliding bubble forms a track; the solution in its volume is mixed. It is assumed that this track, adjacent to the electrode surface, has a length s_1, a width $2\alpha_1 R$ and a height $2\alpha_1 R$, where R is the radius of the sliding bubble and that α_1 is a proportionality factor. The mixed solution within this track has a uniform composition.

Two types of detached bubbles can be distinguished; first, the single bubble which smoothly detaches from its site of attachment to the electrode and then rises at first in the solution near the electrode surface; the coalescence bubble which jumps perpendicularly from the electrode then rises in the solution at some distance from the electrode surface.

A rising detached single bubble also forms a track in which the solution is homogeneously mixed. This track starts from the bubble-detachment site, loses its contact with the electrode surface and moves increasingly away from the electrode surface.

A jumping detached coalescence bubble causes a solution flow near the electrode surface. It is assumed that an electrode surface $\pi\alpha_2^2 R^2$ comes into contact with fresh bulk solution having a bulk concentration of indicator ions, c_b, where α_2 is a proportionality factor and πR^2 is the cross-section of a detached bubble.

To calculate the mass-transfer coefficient of the indicator ion, the following additional assumptions are made:

— the radius, the cross-section and the volume of all departure bubbles are equal;
— the distribution of the bubble-nucleation sites, the bubble tracks and the bubble-departure sites across the electrode surface are uniform;
— the bubble cycle time is equal for all bubbles;
— the bubbles grow on their nucleation sites exclusively;
— the sliding and smoothly detaching single bubbles induce no solution flow within the Prandtl boundary layer at the electrode surface, except the flow necessary to mix the solution of the bubble track;
— the detached coalescence bubbles induce no solution flow within the Prandtl boundary layer at the electrode surface, except the flow necessary to refresh the solution at the electrode surface;
— the bubbles rising outside the Prandtl boundary layer induce a solution flow in the electrolytic cell. This flow is added to the forced flow delivered by a pump, for example. Two extremes are possible, namely either the induced flow or the forced flow can be neglected. Next, we consider the forced flow of solution as dominant;
— the bubble diameter and the height of the bubble track are smaller than the thickness of the Nernst diffusion layer at forced convection, δ_f;
— no effect of migration of indicator ions is considered;
— the concentration of indicator ions at the electrode surface is practically equal to zero; $c_0 < c_b$ or $c_0 = 0$.

2.1. *Sliding bubbles*

First, the mass transfer of indicator ions to the bubble-track part of the electrode surface during the bubble-cycle time t_d has been determined. The concentration profile for the indicator ion at the electrode

surface at forced convection, when no bubble effect is present, is given by the partly dotted curve 1 of Fig. 1. The thickness of the Nernst diffusion layer for an indicator ion at forced convection $\delta_f = D/k_f$, where D is the diffusion coefficient of the indicator ion and k_f is the mass transfer coefficient of the indicator ion. For $0 \leqslant x \leqslant \delta_f$, where x is the distance from the electrode surface, $c_x = xc_b/\delta_f$ and for $x \geqslant \delta_f$ it follows that $c_x = c_b$.

The sliding bubbles make a bubble track with a length s_1 and a width $2\alpha_1 R$ over the electrode surface. The profile of concentration for the bubble track on the electrode surface, directly following the bubble slide, is given by the solid curve 3 of Fig. 1. It can be shown that $c_x = \alpha_1 R\, c_b/\delta_f$ for $0 \leqslant x \leqslant 2\alpha_1 R$, $c_x = x\, c_b/\delta_f$ for $2\alpha_1 R \leqslant x \leqslant \delta_f$ and $c_x = c_b$ for $x \geqslant \delta_f$.

After mixing the solution within the bubble track, the solution in the diffusion layer is regarded as convectionless. The diffusion of indicator ions can be described by the well known Cottrell relation. From the Cottrell relation it follows that the thickness of the Nernst diffusion layer is

$$\delta = \pi^{1/2} D^{1/2} t^{1/2}. \tag{1}$$

It is assumed that, after a time t_s, the concentration profile for indicator ions becomes equal to that at forced convection when no bubble effect is present. Consequently, at $t = t_s$:

$$\delta = \alpha_1 R. \tag{2}$$

From Equations (1) and (2) it follows that:

$$t_s = (\alpha_1 R)^2/\pi D. \tag{3}$$

The average mass-transfer coefficient $k_{s,a}$ during time t_s can be deduced from Cottrell's relation:

$$k_{s,a} = 2(D/\pi t_s)^{1/2}. \tag{4}$$

The number of moles of the indicator ion diffusing to a bubble track on the electrode surface during time t_s is:

$$m_{s,1} = k_{s,a}\, t_s A_s c_x, \quad \text{with } x = \alpha_1 R, \tag{5}$$

where A_s = surface area of a bubble track on the electrode.

$$A_s = 2\alpha_1 R\, s_1 \tag{6}$$

$$c_x = \alpha_1 R\, c_b/\delta_f, \text{ with } x = \alpha_1 R \tag{7}$$

Substitution of A_s and c_x, with $x = \alpha_1 R$, into Equation (5) gives:

$$m_{s,1} = 2k_{s,a} t_s\, \alpha_1^2 R\, s_1^2\, c_b/\delta_f. \tag{8}$$

The number of molecules of the indicator ion diffusing to a bubble track on the electrode surface during the rest of the cycle time $t_d - t_s$ is given by:

$$m_{s,2} = 2k_f (t_d - t_s)\, \alpha_1 R\, s_1 c_b. \tag{9}$$

The mass-transfer coefficient for a bubble track on the electrode surface is schematically given as a function of time in Fig. 2 for two bubble cycles.

The number of moles of the indicator ion diffusing to a bubble track on the electrode surface is given by:

$$m_{s,3} = m_{s,1} + m_{s,2}. \tag{10}$$

Substituting $m_{s,1}$ and $m_{s,2}$ into Equations (8) and (9), respectively, and using $\delta_f = D/k_f$ and Equations (3) and (4), from Equation (10) it can be deduced that:

$$m_{s,3} = 2k_f \alpha_1 R\, s_1\, c_b \left[t_d + \frac{\alpha_1^2 R^2}{\pi D} \right]. \tag{11}$$

2.2. *Jumping detached bubbles*

Only the mass transfer of the indicator ion to that part of the electrode surface is considered which comes into contact with fresh bulk solution after the jump of a bubble. This part of the electrode surface, called the bubble-jump surface, is expressed as:

$$A_w = \pi \alpha_2^2 R^2. \tag{12}$$

It is assumed that, before the bubble detachment the concentration profile for the indicator ion is given by the partly dotted curve 1 of Fig. 1, and directly after the bubble detachment, the concentration of the indicator ion is independent of the distance x to the electrode surface, so that $c_x = c_b$ at $t = 0$ (curve 2). The diffusion of the indicator ions can again be described by the well known Cottrell relation until the concentration profile of the indicator ions has become equal to that given by the partly dotted curve 1 of Fig. 1. The latter profile of concentration is reached after time t_w.

By analogy with t_s and $k_{s,a}$, the relations for t_w and $k_{w,a}$, respectively, can be deduced. These are:

$$t_w = \delta_f^2/\pi D, \tag{13}$$

and:

$$k_{w,a} = 2(D/\pi t_w)^{1/2}, \tag{14}$$

The number of moles of the indicator ion diffusing to

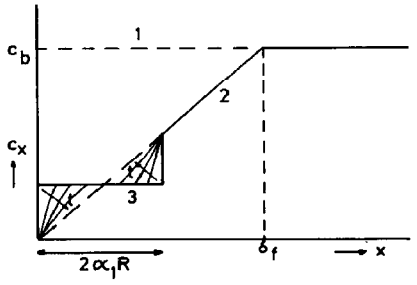

Fig. 1. Profile of indicator-ion concentration for a selected site of electrode at certain periods after the formation of a track by a sliding bubble.

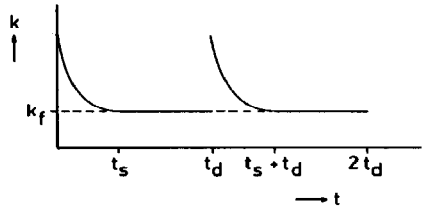

Fig. 2. Mass-transfer coefficient for a bubble track on the electrode surface is schematically given as a function of time for two bubble cycles. The bubble-cycle time is indicated by t_d.

the bubble-jump surface of the electrode during time t_w is:

$$m_{w,1} = k_{w,a}\, c_b\, t_w\, A_w. \tag{15}$$

Where A_w = bubble-jump surface area, we find:

$$A_w = \pi\alpha_2^2 R^2. \tag{16}$$

Substitution of A_w into Equation (15) gives:

$$m_{w,1} = k_{w,a}\, c_b\, t_w\, \pi\alpha_2^2 R^2. \tag{17}$$

The number of moles of the indicator ion diffusing to the bubble-jump surface of the electrode during the rest of the cycle time $t_d - t_w$ is:

$$m_{w,2} = k_f\, c_b\, (t_d - t_w)\, A_w. \tag{18}$$

Substitution of A_w into Equation (18) gives:

$$m_{w,2} = k_f\, c_b\, (t_d - t_w)\, \pi(\alpha_2 R)^2. \tag{19}$$

The number of moles of the indicator ion diffusing to the bubble-jump surface of the electrode during the cycle time t_d is:

$$m_{w,3} = m_{w,1} + m_{w,2}. \tag{20}$$

Using Equations (13), (14), (18) and (19) and $\delta_f = D/k_f$, it can be shown that:

$$m_{w,3} = \alpha_2^2 R^2 c_b \left[\pi k_f t_d + \frac{D}{k_f}\right]. \tag{21}$$

2.3. *Rising detached single bubbles*

When a bubble becomes detached from its site on the surface of the vertical electrode, without the occurrence of coalescence, the bubble slips from the vertical electrode. Immediately after bubble detachment, the distance between the rising bubble and the electrode increases continuously; the trajectory of the bubble is very close to the vertical wall of the electrode that is, within the diffusion layer. Consequently, the bubble will enhance the mass transfer. This bubble also causes a bubble track in which the solution has been mixed. The distance between this bubble track and the electrode increases with increasing distance from the detachment site of the bubble. Profiles of concentration for the indicator ion at various distances are shown in Fig. 3. Fig. 3a gives the profile at the detachment site. The distance from the detachment site increases in sequence, as shown in Figs 3b and c.

No simple mathematical relations are available to calculate the enhancement of mass transfer for the situations represented in Figs 3b and c. Therefore an effective length of bubble track, s_2, for rising detached single bubbles is introduced to describe the enhancement of the mass transfer.

The contribution of the rising detached single bubble to the mass transfer coefficient can be calculated by analogy with the sliding bubble. It is assumed that the width of the track for a rising detached single bubble is $2\alpha_3 R$. It can be shown that the number of moles of the indicator ion diffusing to the electrode surface $A_p = 2\alpha_3 R s_2$ is:

$$m_{p,3} = 2k_f\, \alpha_3 R\, s_2\, c_b \left[t_d + \frac{\alpha_3^2 R^2}{\pi D}\right]. \tag{22}$$

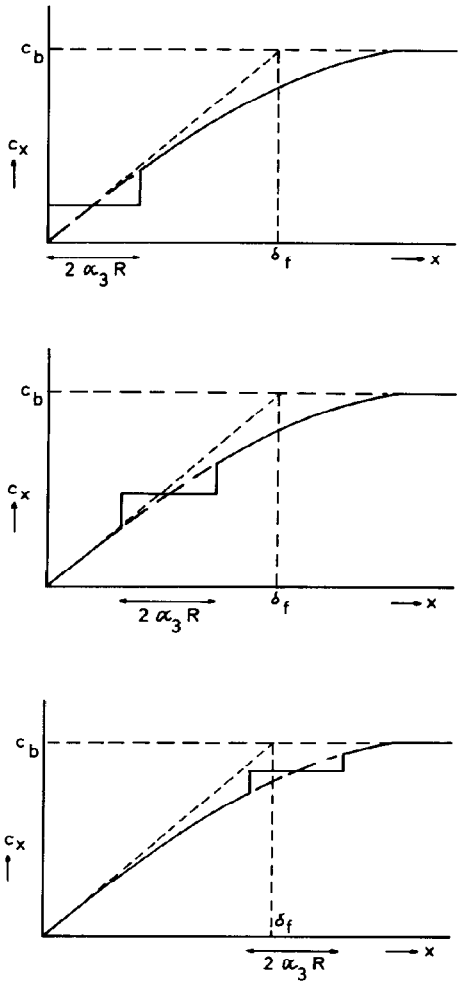

Fig. 3. Profile of indicator ion concentration for selected sites of electrode at different distances from the detachment site of a rising detached single bubble in the direction of its trajectory and as soon as the bubble has been passed.

2.4. *Ensemble of sliding and jumping detached bubbles*

It is assumed that the contributions to the mass transfer of the indicator ion, owing to the bubble slide and the bubble detachment, can be summed. Consequently, the total number of moles of the indicator ion diffusing to the electrode surface, consisting of the surface of the sliding bubble track and that of the bubble detachment, during the bubble cycle time is:

$$m_{sw} = m_{s,3} + m_{w,3}. \tag{23}$$

Substitution of $m_{s,3}$ and $m_{w,3}$ by Equations (11) and (22), respectively, into Equation (23) gives:

$$m_{sw} = 2\alpha_1 R s_1 c_b k_f \left[t_d + \frac{\alpha_1^2 R^2}{\pi D}\right] + \alpha_2^2 R^2 c_b \left[\pi k_f t_d + \frac{D}{k_f}\right]. \tag{24}$$

Using the definition of mass transfer coefficient, k, for the indicator ion, one can show that:

$$k_{sw} = \frac{m_{sw}}{t_d c_b (2\alpha_1 R s_1 + \pi\alpha_2^2 R^2)}. \quad (25)$$

From Equations (24) and (25) it follows that:

$$\frac{k_{sw}}{k_f} = 1 + \frac{2\alpha_1^3 R^2/\pi D + \alpha_2^2 R D/k_f^2}{t_d(2\alpha_1 s_1 + \pi\alpha_2^2 R)}. \quad (26)$$

The enhancement of the mass transfer of the indicator ion due to one sliding and jumping bubble, is given in Equation (26). It is assumed that a gas-evolving electrode can be considered as an ensemble of sliding and jumping bubbles.

From the rate of volumetric gas bubble formation per unit surface area, $v_{g,b}$ and the volume, V_d of a detached bubble, it follows that the number of detached bubbles per unit surface area and time is given by:

$$N = v_{g,b}/V_d. \quad (27)$$

Assuming uniform distributions of bubble tracks and bubble-detachment sites over the electrode surface, the bubble cycle time is given by:

$$t_d = \frac{1}{N(2\alpha_1 R s_1 + \pi\alpha_2^2 R^2)}. \quad (28)$$

From Equations (26–28) and introducing $V_d = 4\pi R^3/3$ it can be shown that the mass transfer coefficient for the indicator ion for the whole electrode is:

$$k = k_f + v_{g,b} k_f \left[\frac{6\alpha_1^3 s_1}{4\pi^2 D} + \frac{3\alpha_2^2 D}{4\pi R k_f^2}\right]. \quad (29)$$

Equation (29) shows that the second term on the right-hand denotes the contribution of sliding bubbles and the third term the contribution of jumping bubbles.

The enhancement factor β is defined by $\beta = (k/k_f) - 1$. Hence:

$$\beta = v_{g,b}\left[\frac{6\alpha_1^3 s_1}{4\pi^2 D} + \frac{3\alpha_2^2 D}{4\pi R k_f^2}\right]. \quad (30)$$

2.5. *Ensemble of sliding bubbles and rising detached single bubbles*

The enhancement of the mass transfer of indicator ions is calculated for an ensemble of sliding and rising detached single bubbles by analogy with the calculation of the enhancement of the mass transfer of indicator ions, resulting from an ensemble of sliding and jumping detached bubbles. It is assumed that the total number of moles of the indicator ion diffusing to the electrode surface of $(2\alpha_1 R s_1 + 2\alpha_3 R s_2)$ during the bubble cycle time t_d is:

$$m_{sp} = m_s + m_p. \quad (31)$$

Based on the definition of mass transfer coefficient, k, for the indicator ion it follows that:

$$k_{sp} = \frac{m_{sp}}{t_c c_b (2\alpha_1 R s_1 + 2\alpha_3 R s_2)}. \quad (32)$$

The bubble cycle time is given by:

$$t_d = \frac{1}{N(2\alpha_1 R s_1 + 2\alpha_3 R s_2)}. \quad (33)$$

It can be shown that the mass transfer coefficient for the indicator ion for the whole electrode is:

$$k = k_f + \frac{3k_f v_{g,b}}{2\pi^2 D}[\alpha_1^3 s_1 + \alpha_3^3 s_2], \quad (34)$$

and the enhancement factor is:

$$\beta = \frac{3 v_{g,b}}{2\pi^2 D}[\alpha_1^3 s_1 + \alpha_3^3 s_2]. \quad (35)$$

3. DISCUSSION

3.1. *Behaviour of bubbles*

In practice, the detached bubbles show a large spread in size. Since the dependence of β on the bubble radius R is related to the ratio between the cross-section and the volume of a bubble, it is advisable to use the average Sauter bubble radius, defined by $R_{s,d} = 3 V_d/4 A_d$, where A_d is the average cross-section of detached bubbles and V_d the average volume of detached bubbles, instead of the average bubble radius R_d, where:

$$R_d = \sum_{i=1}^{n} R_{d,i}/n,$$

$R_{d,i}$ = radius of bubble i and n = the total number of bubbles on a high-speed film strip.

Generally, small bubbles are swept from the electrode surface by a solution flow induced by detached big bubbles, which were present on the electrode as big single bubbles or were formed by coalescence of two or more big bubbles on the electrode.

Single growing bubbles, attached to an electrode surface in a convectionless solution, detach from their nucleation sites when the adhesion force becomes smaller than the buoyancy force, if the electrostatic attraction or repulsion between bubble and electrode can be neglected[11]. The detachment of a single bubble is also affected by the hydraulic force caused by forced solution flow or solution flow induced by the growth of the single bubble and its neighbouring bubbles, the detachment of neighbouring bubbles and the rising of detached bubbles. For a vertical electrode, detached single bubbles rise initially within the diffusion layer at the electrode surface; the distance of a rising bubble to the electrode wall will continuously and slowly increase. A projection of oscillating trajectories of detached single bubbles is given in Fig. 5 of[12].

A bubble departing from its nucleation site on a vertical gas-evolving electrode can also slide over the electrode surface to another site on its surface, after which the bubble smoothly detaches from the electrode surface and starts to rise near the electrode surface.

It is likely that the slide distance increases and the trajectory of a detached single bubble lies closer to the electrode surface with decreasing bubble size.

A coalescence bubble, formed by coalescence of two or more bubbles, strongly vibrates to establish its equilibrium shape and its oscillations end after about half a millisecond[2, 13]. The series of interesting frames, made by Sides and Tobias[13], clearly show the coalescence of bubbles and the behaviour of the

resulting bubble on detachment from and return to the electrode. Probably, in this case, the coalescing bubbles are too small to form a definitively detached coalescence bubble[4].

About 15 years ago, high-speed films were made of an oxygen- and a hydrogen-evolving vertical 2 mm high platinum electrode in 1 M H_2SO_4. The coalescence of two oxygen bubbles, a 0.48 mm diameter and a 0.37 mm diameter bubble, present on the underside of a 0.1 mm thick platinum electrode and the behaviour of the resulting coalescence bubble were filmed by a high-speed camera at the rate of 6000 pictures per second. A series of frames is shown in Fig. 4.

The last frame before the start of coalescence is indicated by number 1. The number of the other frames indicates the frame number on the film strip after frame 1. After the start of coalescence of the two big bubbles, the coalescence bubbles compress along the axis of coalescence. Its shape changes completely arbitrarily for about 3 ms. The centre of the coalescence bubble moves downwards, where the distance from the surface of the coalescence bubble to the underside of the vertical electrode is about 0.027 mm, when the bubble rises because of the buoyancy force and attaches again to the underside of the vertical electrode. Owing to the arbitrary changes in shape, the distance between the surface of the coalescence bubble and the electrode surface also changes arbitrarily, despite the more or less continuously increasing distance between the centre of the bubble and the electrode surface. The return of the coalescence bubble from Fig. 4 is caused by the buoyancy force exerted upon the bubble.

Sides and Tobias[13] have, in the case of the vertical wall of an electrode, also observed the return of a coalescence bubble to the electrode surface. They have mentioned three possible causes, *viz* the attraction of the charged bubble to the electrode surface[14, 15], the occurrence of a surface tension gradient[16] and the occurrence of oscillations where one part of the coalescence bubble touches the electrode[13]. From Fig. 4 it can be concluded that the return of the coalescence bubble, observed by Sides and Tobias, can be well explained by the third possibility, *viz* the change in shape of the coalescence bubble.

From Fig. 4 it follows that about 0.003 s after the start of coalescence the maximum distance between the coalescence bubble and the underside of the electrode has been reached, *viz* 0.027 mm. Assuming a linear decrease in the velocity of the downwards-moving bubble, it can be estimated that the coalescence bubble jumps with a velocity of about 0.16 m s^{-1}, perpendicularly from the underside of the electrode. Clearly, coalescence of bubbles, certainly when detachments of the resulting bubbles occur, induce a strong flow of the solution near the electrode surface and cause considerable enhancement of the mass transfer at the gas-evolving electrode.

3.2. *Mass transfer*

To describe the mass transfer of indicator ions to a gas-evolving electrode under conditions of natural convection, Venczel[17], a co-worker of Ibl, has proposed the first penetration model. This model has further been developed by Ibl and Venczel[18] and Janssen[4]. A microconvection model, introduced by Vogt[19] takes into account the effect of the solution flow caused by growing bubbles. A hydrodynamic or macroconvection model[5] considers the effect of the solution flow caused by a swarm of bubbles rising near the electrode surface. In practice, forced convection of solution in an electrolytic cell with gas-evolving electrodes caused by mechanical pumping is often applied to enhance the mass transfer to gas-evolving electrodes and/or to reduce the ohmic potential drop by removing quickly the bubbles from the interelectrode gap. Some models have been modified for describing the mass transfer to a gas-evolving electrode under conditions of forced convection[3, 20]. Janssen and Barendrecht[3] present a model in which exclusively detached bubbles are taken into account. Comparison of Equation (28) in this paper with Equation (16) in[3] indicates that both equations are identical when bubbles do not slide over the electrode surface and the proportionality factor a_d in[3] is equal to α_2^2 as in the present paper.

3.2.1. *Oxygen-evolving electrode in alkaline solution.* For an oxygen-evolving electrode in alkaline solution under natural convection conditions, log k/log i_0 curves show two current-density regions differing quite considerably in slope. A gradual one, *viz* about 0.3, at $i_0 < 0.10$ kA m^{-2} and a steep one, *viz* about 0.9, at $i_0 > 0.10$ kA m^{-2} corresponding to, respectively, the occurrence or nonoccurrence of coalescence of gas bubbles[21].

In the high current-density region, practically all the detached big bubbles are coalescence bubbles and jump perpendicularly from the electrode surface. Practically no oxygen bubbles slide over the electrode surface. The detached coalescence bubbles rise beyond the diffusion layer, and have then practically no effect upon the mass transfer at the electrode. An ensemble of rising bubbles in the bulk of solution does induce an additional flow of solution in the cell. Generally, this flow can be neglected at forced convection. The solution flow at the electrode surface, induced by detached coalescence bubbles, is much more vigorous than that induced by detached single bubbles. This means that the factor α_2 from Equation (12) for a detached coalescence bubble is much larger than α_3 for a detached single bubble.

For a gas-evolving electrode, where practically no slip of bubbles occurs, Equations (28) and (29) can be reduced to, respectively:

$$k = k_f + \frac{3 v_{g,b} \alpha_2^2 D}{4 \pi R k_f}, \tag{36}$$

and:

$$\beta = \frac{3 v_{g,b} \alpha_2^2 D}{4 \pi R k_f^2}. \tag{37}$$

In previous work[3] Equation (36) has been thoroughly checked for an oxygen-evolving electrode in alkaline solution at forced convection and a current density range where the increase in the mass transfer coefficient k is proportional to $i_0^{0.85}$. It has been found that Equation (36) can be used successfully to describe the mass-transfer coefficient k and that the factor $\alpha_2 = 1.3$.

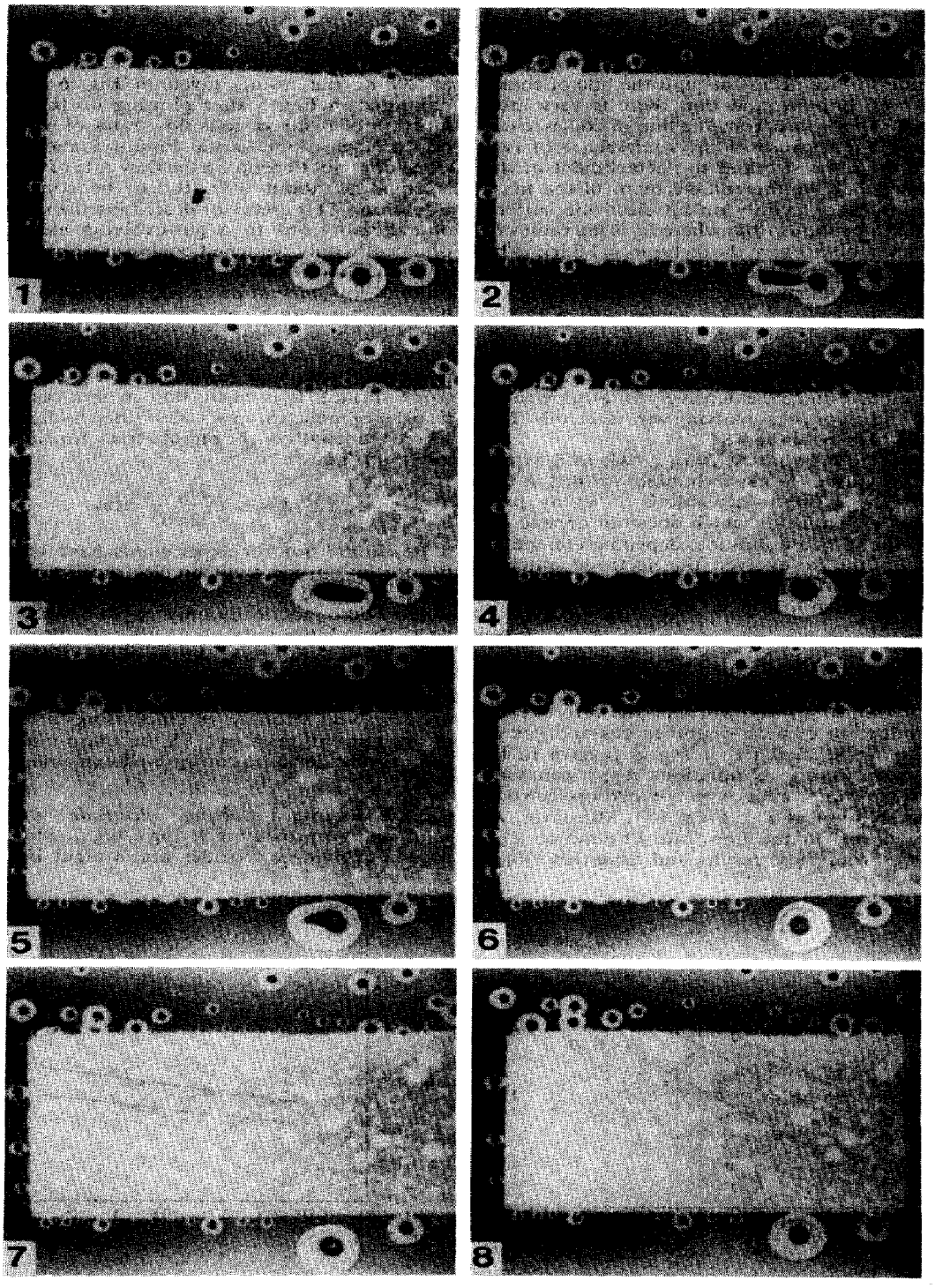

Fig. 4. Coalescence of two bubbles, attached to the underside of a vertical 2 mm high platinum electrode: (1) picture at $t = 0$; (2) 0.33 ms; (3) 0.5 ms; (4) 0.83 ms; (5) 1.5 ms; (6) 2.0 ms; (7) 3.66 ms; (8) 4 ms. Conditions: 6000 frames per second, oxygen evolution; 313 K; no forced convection; 1 M H_2SO_4 and 5 kA m^{-2}.

Very sophisticated experiments by Dees and Tobias[10] have shown that after coalescence and disengagement of 500 and 540 μm diameter bubbles a strong increase of mass transfer of an indicator ion to the electrode surface occurs around the line of coalescence of both bubbles and that there is very little effect 500–600 μm away from the line of coalescence. This means that because of the coalescence of two bubbles of the same size and the detachment of the newly formed bubble, the enhancement of the mass transfer takes place mainly on an electrode surface area smaller than about $10R_d^2$ where R_d is the radius of the detached bubble. From the factor $\alpha_2 = 1.3$ it can be calculated that the bubble-jump surface of the electrode A_w is $5.3\,R_d^2$. Comparing both areas of surface it follows that the factor $\alpha_2 = 1.3$ agrees well with the sphere of influence of coalescing bubbles[10]. Recently, the dependence of the average Sauter bubble radius, $R_{s,a}$, and the efficiency of gas-bubble evolution, η_b, have been investigated extensively for a chlorine-, a hydrogen- and an oxygen-evolving wire electrode. The results have been published[8].

It has been found that $R_{s,d} = a_1 i_b^{n_1}$ where i_b is the current density used for gas in bubbles formed at the electrode, a_1 is a factor depending on many parameters and n_1 is a factor which does not depend on the rate of solution flow, but does depend on temperature, nature of the gas evolved, the electrode material and electrolyte[8]. The dependence of efficiency of gas bubble evolution on i_b is given by:

$$\eta_b/(1-\eta_b) = a_2 i_b^{n_2}, \tag{38}$$

where a_2 is a factor determined by many parameters such as the nature of the gas evolved and rate of solution flow. Since $\eta_b = i_b/i$ where i is the current used for the production of both dissolved gas and gas in bubbles, it can be shown that k and β have to be described by very complex equations. Approximately, η_b is almost constant for an oxygen-evolving electrode in alkaline solution at $i > 2$ kA m^{-2}[8]. Moreover, n_1 does not depend on the flow rate of solution and $n_1 = 0.21$[8]. From these results and Equation (30) it can be shown that the difference $k-k_f$ is proportional to $i^{0.79}$. This dependence agrees well with the experimental one[9, 17].

For an oxygen-evolving electrode in 1 M KOH and at 298 K, the results given in Fig. 6 from[9] are presented in Fig. 5 after plotting $\beta = (k-k_f)/k_f$ as a function of i_0 for various flow rates of solution on a double logarithmic scale. Figure 5 shows that the slope does not depend on the flow rate of solution and is equal to about 0.72. It can be concluded that Equation (37) is useful for describing the mass transfer of indicator ions to a gas-evolving electrode with practically only detached coalescence bubbles.

For an oxygen-evolving electrode in alkaline solution at low current densities, *viz* $i_0 < 0.1$ kA m^{-2} at natural convection, practically all the bubbles are single bubbles smoothly detached from the electrode surface. Practically all the bubbles detach from their nucleation sites and also definitively from the electrode surface. It is likely that in this case the mass transfer of indicator ions is described by Equation (34) where the length of the bubble-track for sliding bubbles $s_1 = 0$. Thus:

$$k = k_f + \frac{3\,k_f v_{g,b}}{2\pi^2 D}\alpha_3^2 s_2. \tag{39}$$

Few mass transfer experiments have been carried out for an oxygen-evolving electrode in alkaline solution at forced convection and in a current density range where practically only single bubbles are evolved. By plotting k *vs* i_0, k_e is determined at $i_0 = 0$ kA m^{-2} by extrapolation of the k/i_0 curve. It has been found that k_e at $i_0 = 0$ kA m^{-2} is only slightly higher than k_f[9]. Since $v_{g,b}$ is proportional to i_b and i_b increases very strongly with increasing current density at low current densities i[8], the sharp incline of k at low current densities can be well explained.

3.2.2. *Hydrogen-evolving electrode in alkaline solution.* Approximately, $\log k/\log i_H$ plots for hydrogen-evolving electrodes are straight lines with a

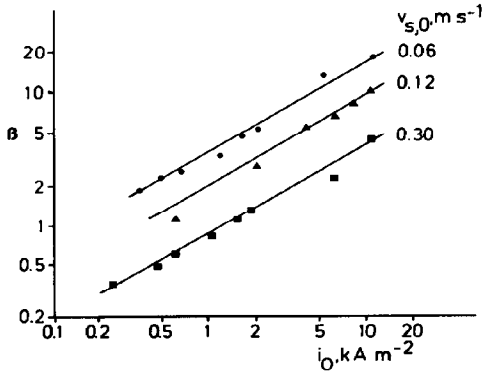

Fig. 5. Mass-transfer enhancement factor for mass transfer of indicator ions is plotted as a function of i_0 on a double logarithmic scale for an oxygen-evolving electrode in alkaline solution at various rates of solution flow and 298 K. Data obtained from Fig. 6 in[9].

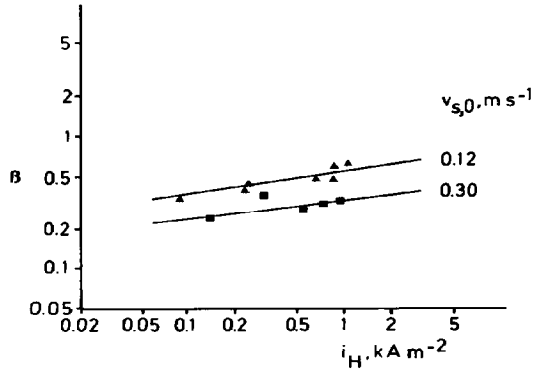

Fig. 6. Enhancement factor for mass transfer of indicator ions is plotted as a function of i_H on a double logarithmic scale for a hydrogen-evolving electrode in alkaline solution at various rates of solution flow and 298 K. Data obtained from Fig. 5 in[9].

slope of usually about 0.3. Only for electrode materials like Ni/Teflon on which very big coalescence bubbles are evolved, a rather higher slope, that is 0.7 has been found. This type of hydrogen-evolving electrode is not taken into consideration.

Plotting k as a function of i_H, the resulting curve is practically also a straight line, even from very low i_H, *viz* 0.04 kA m^{-2} at a solution flow rate of 0.12 m s^{-1}[9]. Linear extrapolation to $i_H = 0$ kA m^{-2} gives k_e at $i_H = 0$ kA m^{-2}. It has been found that for solution flow rates less than 0.36 m s^{-1} k_e is much larger than k_f.

The bubble behaviour for a hydrogen-evolving electrode in alkaline solution is characterized by sliding and detaching single bubbles. Consequently, the mass transfer coefficient for indicator ions is given by Equation (34). In the range of low current densities, it is likely that the factors α_1 and α_3, the length of the sliding bubble track s_1 and the effective length of the bubble track s_2 for rising detached single bubbles are practically independent of current density. It has been found that the efficiency of bubble evolution and thus $v_{g,b}$ as well, increases sharply with increasing current density at low $i < 0.1$ kA m^{-2} at a solution flow rate of 0.12 m s^{-1}[7]. The strong increase in k may be explained very well, taking into account the strong increase in the efficiency of bubble evolution. A similar effect, though clearly smaller, has been found for oxygen-evolving electrodes at low current densities[3, 9].

In the range of high current densities, the mass transfer coefficient k for indicator ions increases slowly with increasing current density. The efficiency of bubble evolution for a hydrogen-evolving electrode in 1 M KOH at 298 K is almost constant above 0.5 kA m^{-2}[8]. Based on the behaviour of hydrogen bubbles at high current densities, Equation (35) is used to describe the mass transfer of indicator ions. The enhancement factor $\beta = (k - k_f)/k_f$ is plotted as a function of i_H on a double logarithmic scale in the experiments for which results are given in Fig. 6 of[9]. Figure 6 shows that the slope of the log β/log i_H curve is practically independent of the flow rate of solution, as found for oxygen-evolving electrodes (see Fig. 5), and is flat, *viz* 0.14, and that the enhancement factor β decreases with increasing flow rate of solution.

It has been found that at high current densities the efficiency of gas bubble evolution increases slowly with increasing current density and decreases slowly with increasing flow rate of solution[8]. For the experimental conditions of Fig. 6, the efficiency of gas bubble evolution is practically constant. From Fig. 6 and using Equation (35) it follows that the factor $\alpha_1^3 s_1 + \alpha_3^3 s_2$ decreases strongly with increasing current density, *viz* $\alpha_1^3 s_1 + \alpha_3^3 \alpha_2$ is inversely proportional to $i_H^{0.86}$ and decreases with increasing flow rate of solution. It has been found that the size of detached bubbles increases with increasing current density, that is $R_{s,d}$ is proportional to $i_H^{0.26}$, and decreases with increasing flow rate of solution, in other words, $R_{s,d}$ is proportional to $v_s^{-0.08}$, hence, it is likely that the factor $\alpha_1^3 s_1 + \alpha_3^3 s_2$ decreases with decreasing size of detached bubbles.

Dees and Tobias[10] have found that an increase in mass transfer of indicator ions to segments of the electrode is relatively small after disengagement of a single bubble from a horizontal electrode. It is thus advisable to take into account the slide of a bubble and the trajectory of a rising bubble near the electrode surface to describe the enhancement of the mass transfer of indicator ions.

A model analogous to that for an ensemble of sliding bubbles and rising detached single bubbles, is also useful to describe the enhanced mass transfer caused by small solid particles dispersed in a solution or by droplets emulsified in a solution.

REFERENCES

1. H. Vogt, in *Comprehensive Treatise of Electrochemistry* (Edited by E. Yeager, J. O'M. Bockris, B. E. Conway and S. Sarangapani), vol. 6, p. 445, Plenum Press, New York (1983).
2. P. J. Sides, in *Modern Aspects of Electrochemistry* (Edited by R. E. White, J. O'M. Bockris and B. E. Conway), vol. 13, p. 303, Plenum Press, New York (1986).
3. L. J. J. Janssen and E. Barendrecht, *Electrochim. Acta* **30,** 683 (1985).
4. L. J. J. Janssen and S. J. D. van Stralen, *Electrochim. Acta* **26,** 1011 (1981).
5. L. J. J. Janssen and E. Barendrecht, *Electrochim. Acta* **24,** 693 (1979).
6. L. J. J. Janssen, *J. appl. Electrochem.* **17,** 1177 (1987).
7. J. M. Chin Kwie Joe, L. J. J. Janssen, S. J. D. van Stralen, J. H. G. Verbunt and W. M. Sluijter, *Electrochim. Acta*, accepted.
8. J. M. Chin Kwie Joe, L. J. J. Janssen, S. J. D. van Stralen, J. H. G. Verbunt and W. M. Sluijter, *Electrochim. Acta* **33,** 769 (1988).
9. L. J. J. Janssen and E. Barendrecht, *Dechema-Monogr.* 463 (1985).
10. D. W. Dees and C. W. Tobias, *J. electrochem. Soc.* **134,** 1702 (1987).
11. B. Kabanov and A. Frumkin, *Z. Chem.* **165,** 433 (1933).
12. L. J. J. Janssen and J. G. Hoogland, *Electrochim. Acta* **15,** 1013 (1970).
13. P. J. Sides and C. W. Tobias, *J. electrochem. Soc.* **132,** 583 (1985).
14. A. Coehn, *Z. Elektrochem.* **29,** 1 (1923).
15. A. Coehn and H. Neumann, *Z. Phys.* **20,** 54 (1923).
16. J. P. Glas and J. W. Westwater, *Int. J. Heat Mass Transfer* **7,** 1427 (1964).
17. J. Venczel, Thesis, ETH Zürich (1961).
18. N. Ibl and J. Venczel, *Metalloberfläche* **24,** 365 (1970).
19. H. Vogt, Thesis, University of Stuttgart (1977).
20. H. Vogt, *Electrochim. Acta* **32,** 633 (1987).
21. L. J. J. Janssen, *Electrochim. Acta* **23,** 81 (1978).